

Anisotropic electrical spin injection in ferromagnetic semiconductor heterostructures

著者	Young D. K., Johnston-Halperin E., Awschalom D. D., Ohno Y., Ohno H.
journal or publication title	Applied Physics Letters
volume	80
number	9
page range	1598-1600
year	2002
URL	http://hdl.handle.net/10097/51787

doi: 10.1063/1.1458535

Anisotropic electrical spin injection in ferromagnetic semiconductor heterostructures

D. K. Young, E. Johnston-Halperin, and D. D. Awschalom^{a)}

Center for Spintronics and Quantum Computation, University of California, Santa Barbara, California 93106

Y. Ohno and H. Ohno

Laboratory for Electronic Intelligent Systems, Research Institute of Electrical Communication, Tohoku University, Katahira 2-1-1, Aoba-ku, Sendai 980-8577, Japan

(Received 15 November 2001; accepted for publication 9 January 2002)

A fourteen-fold anisotropy in the spin transport efficiency parallel and perpendicular to the charge transport is observed in a vertically biased (Ga, Mn)As-based spin-polarized light emitting diode. The spin polarization is determined by measuring the polarization of electroluminescence from an (In, Ga)As quantum well placed a distance d (20–420 nm) below the p -type ferromagnetic (Ga, Mn)As contact. In addition, a monotonic increase (from 0.5% to 7%) in the polarization is measured as d decreases for collection parallel to the growth direction, while the in-plane polarization from the perpendicular direction ($\sim 0.5\%$) remains unchanged. © 2002 American Institute of Physics. [DOI: 10.1063/1.1458535]

Understanding the physical mechanisms underlying the manipulation of electronic spin in semiconductors may ultimately lead to multifunctional devices based on photonics, electronics, and magnetics.¹ Moreover, utilizing coherent spin phenomena in semiconductors² may be fundamental for the future of quantum computation in the solid state. The demonstrations of electrical spin injection into semiconductors using both ferromagnetic³ and paramagnetic semiconductors,⁴ and more recently with Zener tunneling processes^{5,6} are promising for potential spin based electronics.

Here we report a fourteen-fold anisotropy in the electrical spin injection efficiency between directions parallel and perpendicular to the current flow along the growth axis in a spin-polarized light emitting diode,³ demonstrating the importance of device geometry in obtaining efficient injection and detection. Under forward bias, spin-polarized holes^{7,8} from (Ga, Mn)As and unpolarized electrons from an n -type GaAs substrate are injected into an embedded (In, Ga)As quantum well (QW) separated from the ferromagnetic region by a spacer layer d (20–420 nm). Spin polarization of the electrically injected holes is measured by analyzing the polarization (P) of the emitted electroluminescence (EL) either along the growth direction (through the substrate) or in plane (from a cleaved facet). In addition, we find that as the spacer layer thickness decreases, the magnitude of EL polarization monotonically increases from 0.5% to 7% when the hole spin orientation is along the direction of charge transport (growth direction). In contrast, EL polarization is insensitive to spacer layer thickness when measured in the plane of the sample ($P \sim 0.5\%$ for all d), where the hole spin orientation is perpendicular to the charge transport. This spacer layer dependence is not intrinsic to the QW, but arises from a difference in spin transport efficiency for the two geometries.

The device structure shown in the inset of Fig. 1(a) is

grown by molecular-beam epitaxy on a (100) n -GaAs substrate with a 500 nm n^+ -GaAs buffer layer (doping density $N_D = 2 \times 10^{18} \text{ cm}^{-3}$) and the following layers: 20 nm undoped GaAs, 10 nm undoped $\text{In}_{0.12}\text{Ga}_{0.88}\text{As}$ strained QW, undoped GaAs spacer with thickness d (20, 70, 120, 220, or 420 nm), and 300 nm $\text{Ga}_{1-x}\text{Mn}_x\text{As}$ with $x = 0.045$ or 0.035 . Details of the growth of the magnetic layer can be found elsewhere.⁹ The epitaxial wafer is processed into light emitting devices having 150 μm -wide mesa stripes defined by wet chemical etching after metal electrode deposition (5 nm Ti/250 nm Au) and cleaved into $\sim 1 \text{ mm} \times 5 \text{ mm}$ pieces. Both p and n contacts are made from the top allowing EL collection from a cleaved facet or through the substrate [Fig. 1(a)]

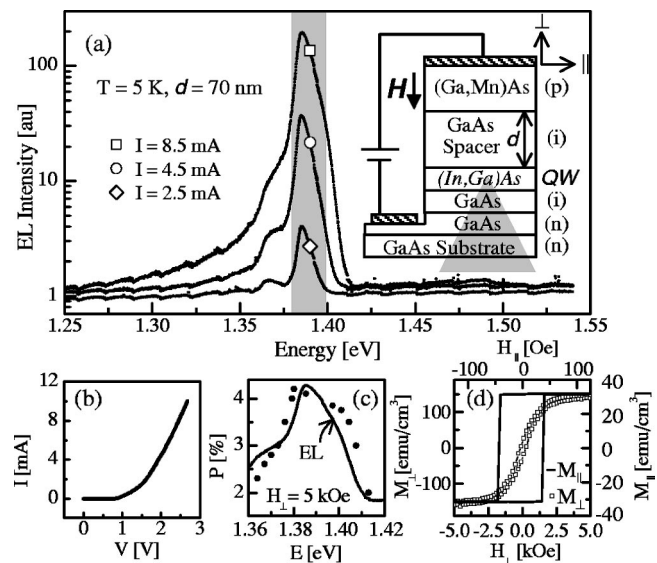


FIG. 1. (a) Spectrally resolved EL intensity along the growth direction for several bias currents, I . Inset shows device schematic and EL collection geometries. (b) I - V characteristic. (c) EL intensity (solid curve) and polarization (\bullet) at $H_{\perp} = 5 \text{ kOe}$ showing a peak in the polarization at the QW ground state ($E = 1.39 \text{ eV}$). (d) Magnetic characteristics of an unprocessed part of the sample when applying a field perpendicular (open squares) and parallel (solid curve) to the sample plane (note the different field scales).

^{a)}Electronic mail: awsch@physics.ucsb.edu

inset]. Two sets of control samples are prepared to verify spin injection, (1) a nonmagnetic device ($d=20$ nm) with a p -type GaAs:Be layer ($p=2 \times 10^{18}$ cm $^{-3}$) substituted for the (Ga, Mn)As layer and (2) a magnetic structure ($d=100$ nm) without metal contacts enabling resonant optical excitation of the QW.

The samples are mounted in a magneto-optical cryostat with a variable magnetic field, applied in or out of plane that is monitored by *in situ* Hall bars. For both cases, EL is collected along the applied field axis. The polarization $P=(I^+ - I^-)/(I^+ + I^-)$ of the EL spectra is analyzed with a variable wave plate and linear polarizer, and is detected with a charge coupled device attached to a 1.33 m spectrometer. Here I^+ and I^- are intensities of the right- and left-hand side circularly polarized components of the EL, respectively.

Figures 1(a)–1(c) show the optical and electrical characteristics at $T=5$ K for a device with $d=70$ nm. Figure 1(a) shows the EL intensity as a function of energy for different bias conditions and its current–voltage (I – V) curve is shown in Fig. 1(b). Moreover, the (In, Ga)As QW emission is spectrally distinct ($E=1.39$ eV) from that of the GaAs heterostructure ($E=1.51$ eV) allowing one to study the depth of spin injection with varying spacer layer.^{3,4} Figure 1(c) shows the polarization (●) and EL intensity (solid curve) as a function of energy with an out-of-plane magnetic field H_{\perp} (~ 5 kOe). Peaks in the EL intensity [full width at half maximum (FWHM)=10 meV] and polarization coincide with the QW ground-state emission energy indicating that spin-polarized holes are injected into the QW. We observe minimal dependence of the polarization on the injection current density,³ allowing us to drive the device for optimal signal to noise. Finally, we characterize the magnetization of the (Ga, Mn)As layer at $T=5$ K by superconducting quantum interference device (SQUID) magnetometry [Fig. 1(d)] confirming that easy and hard magnetization axes of the (Ga, Mn)As layer are in and out of the sample plane, respectively.⁹

Figure 2(a) shows relative changes in EL polarization¹⁰ $\Delta P \equiv P - P_{\text{background}}$, as a function of magnetic field (H_{\perp}) for various temperatures near and below the Curie temperature (T_C). Below $T=62$ K, ΔP saturates around $H_{\perp} \sim 2.5$ kOe, tracking the magnetization of the (Ga, Mn)As shown in Fig. 1(d). The saturation polarization P_S decreases and ultimately vanishes as the temperature increases from $T=5$ to 62 K, commensurate with the temperature dependent magnetization measured by the SQUID (inset). The deviation from mean field theory of $M(T)$ is consistent with previous studies.^{7,8}

The nonmagnetic device verifies that the field dependence of the polarization is due to spin injection rather than Zeeman splitting induced by stray fields from the (Ga, Mn)As. In contrast to the magnetic devices, the EL polarization from the nonmagnetic device [Fig. 2(b)] does not show saturating behavior as a function of field, revealing only the Zeeman contributions in the QW polarization¹⁰ ($P=0.5\%$ at $H_{\perp}=5$ kOe). This indicates that Zeeman splitting in the QW from the applied field as well as the local fields from the (Ga, Mn)As layer ($H_{\text{stray}} \sim 500$ Oe)⁹ are unlikely to be responsible for the saturating polarization in the magnetic structures.

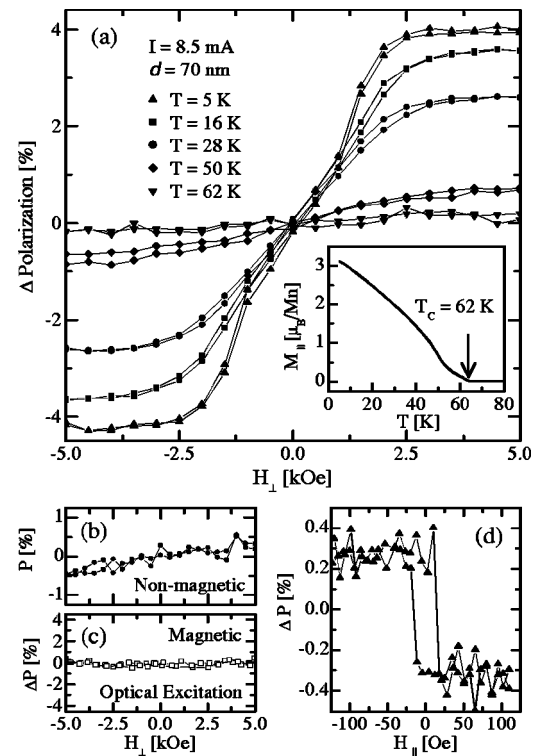


FIG. 2. (a) Temperature dependence of the relative changes in the energy-integrated [gray shaded area in Fig. 1(a)] polarization ΔP as a function of out-of-plane magnetic field. When $T < 62$ K, polarization saturates at $H_{\perp} \sim 2.5$ kOe, commensurate with Fig. 1(d). Inset shows $M(T)$, indicating that the polarization is proportional to magnetic moment. The absence of saturating polarization at $T=5$ K from a (b) nonmagnetic device and from a (c) magnetic structure under optical excitation. (d) Hysteretic EL polarization as a function of *in-plane* magnetic field reveals anisotropic spin injection efficiency giving rise to a magnitude difference and sign flip.

Since (Ga, Mn)As exhibits strong magnetic circular dichroism (MCD),⁸ it is also important to confirm that the observed saturating polarization is not due to preferential reabsorption of QW luminescence passing through the (Ga, Mn)As layer. A magnetic sample without metal contacts is prepared, allowing resonant optical excitation of unpolarized carriers into the QW in the same measurement geometry as used for the EL. A p -type layer between the QW and a semi-insulating substrate is incorporated into the structure in order to reduce the electrostatic potential across the junction, thus leading to more efficient radiative recombination. A pulsed Ti:Sapphire laser (FWHM ~ 20 meV) is used to create *unpolarized* carriers in the QW by illuminating through the cleaved facet with linearly polarized light at $E=1.401$ eV, 56 meV above the QW ground state, and ~ 100 meV below the GaAs band gap. The photoluminescence polarization as a function of magnetic field shown in Fig. 2(c) reveals no saturation, suggesting that the EL polarization does not originate from MCD effects.

Optical selection rules responsible for the QW luminescence¹¹ suggest that the measured spin polarization depends on collection geometry. By rotating the sample 90°, we measure from the cleaved edge, and observe hysteretic EL polarization [shown in Fig. 2(d)], reflecting the *in-plane* magnetic properties of the (Ga, Mn)As layer³ [Fig. 1(d)]. However, the spin polarization is a factor of 10 smaller than out of plane, and exhibits an overall minus sign in the field dependence. Due to quantum confinement and strain, the an-

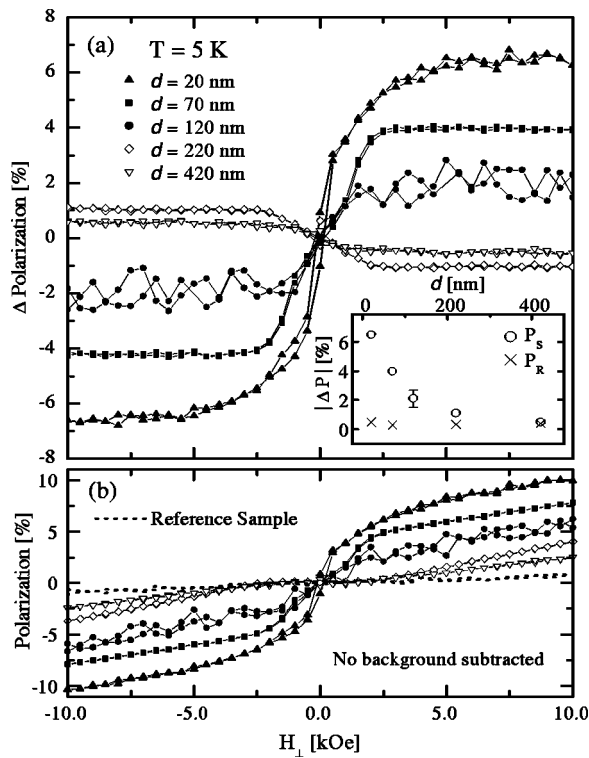


FIG. 3. (a) Spacer layer dependence of EL polarization as function of out-of-plane field. Inset compares the magnitude of the polarization collected both in (ΔP_R) and out-of-plane (ΔP_S) as a function of spacer layer thickness. As d decreases ΔP_S monotonically increases from 0.5% to 7%, while ΔP_R remains unchanged. (b) All samples plotted without the background subtracted reveals Zeeman and strain related contributions. All magnetic samples have similar slopes suggesting spin injection anisotropy is not due to selection rule enhancement or strain.

gular momentum of the heavy hole (HH) is pinned along the growth direction, and in plane for the light hole (LH).¹¹ Therefore, nonzero polarization from both in- and out-of-plane geometries suggests a contribution from both spin-polarized HH and LH to the EL. Similar behavior has also been observed in spin-polarized Zener tunneling diodes.⁵

In an attempt to determine whether the polarization anisotropy depends on a difference in spin transport efficiency or is an intrinsic property of the QW, a set of samples with varying spacer layer thickness ($d = 20$ –420 nm) was studied [shown in Fig. 3(a)]. As the magnetic layer is placed closer to the QW, the magnitude of the EL saturation polarization ΔP_S increases from 0.5% to 7% when the hole spin is oriented along the charge transport direction (growth direction). In contrast, when the hole spin is oriented orthogonal to charge transport, the magnitude of the remanent EL polarization remains constant ($\Delta P_R \sim 0.5\%$) over the range of spacer layer thickness [inset of Fig. 3(a)], consistent with earlier measurements.³ If the factor of fourteen enhancement was intrinsic to the QW, the two orientations would have a similar spacer layer dependence. Also, note that the sign of the out-of-plane polarization flips when the spacer layer d is greater than 220 nm. This effect is also seen in the in-plane polarization, preserving the overall minus sign between the

two orientations (not shown). Due to its spacer layer dependence, the sign flip for the $d > 200$ nm devices suggest that its origin may be intrinsic to spin transport and is unlikely due to spin injection processes.

Further insight into the mechanism underlying the anisotropy is obtained by considering the background polarization from the EL. We plot the polarization data for all of the samples without the linear background subtracted to investigate the possibilities that the spacer layer dependence is due to modulation of the strain from the overlaying magnetic layer [Fig. 3(b)]. As mentioned earlier, the linear slope of the field dependence of the polarization is due to Zeeman and strain contributions.¹² Clearly, the slope of the linear background is very similar for all the samples (even for $d > 200$ nm) and shows no systematic variation as a function of spacer thickness, suggesting that the effects of strain are not the cause of the anisotropy. In addition, the nonmagnetic reference sample has a different slope than the magnetic samples, supporting our assumption that the slope is sensitive to strain. Thus, the spacer layer dependence of the anisotropic spin injection efficiency and the sign flip at larger d (> 200 nm) are not likely caused by strain variation in the sample set. While the mechanism is still unclear, we propose that this anisotropy could arise from either or the combination of the following: (1) anisotropy in the spin polarization of (Ga, Mn)As, (2) differing spin scattering mechanisms for HH versus LH, or (3) spin scattering mechanisms that depend on spin orientation relative to the transport direction.¹³

The authors thank D. R. Schmidt and J. A. Gupta for technical support as well as P. A. Crowell, R. K. Kawakami, and R. J. Epstein for helpful discussions. The work at UCSB was supported by the AFOSR (F49620-99-1-0033), NSF (DMR-0071888), and DARPA/ONR (N00014-99-1-1096). The Japan Society for the Promotion of Science and the Ministry of Education support the work done at Tohoku.

¹S. A. Wolf, D. D. Awschalom, R. A. Buhrman, J. M. Daughton, S. von Molnár, M. L. Roukes, A. Y. Chtchelkanova, and D. M. Treger, *Science* **294**, 1488 (2001) and references therein.

²D. D. Awschalom and J. M. Kikkawa, *Phys. Today* **52**, 33 (1999).

³Y. Ohno, D. K. Young, B. Beschoten, F. Matsukura, H. Ohno, and D. D. Awschalom, *Nature (London)* **402**, 790 (1999).

⁴R. Fiederling, M. Keim, G. Reuscher, W. Ossau, G. Schmidt, A. Waag, and L. W. Molenkamp, *Nature (London)* **402**, 787 (1999).

⁵E. Johnston-Halperin, D. Lofgreen, R. K. Kawakami, D. K. Young, L. Coldren, A. C. Gossard, and D. D. Awschalom, *Phys. Rev. B* **64**, R041306 (2002).

⁶M. Kohda, Y. Ohno, K. Takamura, F. Matsukura, and H. Ohno, *Jpn. J. Appl. Phys., Part 2* **40**, L1274 (2001).

⁷H. Ohno, *Science* **281**, 951 (1998).

⁸B. Beschoten, P. A. Crowell, I. Malajovich, D. D. Awschalom, F. Matsukura, A. Shen, and H. Ohno, *Phys. Rev. Lett.* **83**, 3073 (1999).

⁹H. Ohno, A. Shen, F. Matsukura, A. Oiwa, A. Endo, S. Katsumoto, and Y. Iye, *Appl. Phys. Lett.* **69**, 363 (1996).

¹⁰Background polarization is linear in field and its slope reflects both Zeeman and strain related contributions.

¹¹S. A. Crooker, D. D. Awschalom, J. J. Baumberg, F. Flack, and N. Samarth, *Phys. Rev. B* **56**, 7574 (1997).

¹²G. Hendorfer and J. Schneider, *Semicond. Sci. Technol.* **6**, 595 (1991).

¹³S. J. Papadakis, E. P. De Poortere, M. Shayegan, and R. Winkler, *Phys. Rev. Lett.* **84**, 5592 (2000).